Target Guided Synthesis of 5-Benzyl-2,4-diamonopyrimidines: Their Antimalarial Activities and Binding Affinities to Wild Type and Mutant Dihydrofolate Reductases from *Plasmodium falciparum*

Chawanee Sirichaiwat,[†,‡] Chakapong Intaraudom,[†] Sumalee Kamchonwongpaisan,[†] Jarunee Vanichtanankul,[†] Yodhathai Thebtaranonth,*[,†,‡] and Yongyuth Yuthavong[†]

National Center for Genetic Engineering and Biotechnology, National Science and Technology Development Agency, 113 Thailand Science Park, Pahonyothin Road, Klong 1, Klongluang, Pathumtani 12120, Thailand, and Department of Chemistry, Faculty of Science, Mahidol Univerity, Rama 6 Road, Bangkok 10400, Thailand

Received July 11, 2003

The resistance to pyrimethamine (PYR) of *Plasmodium falciparum* arising from mutation at position 108 of dihydrofolate reductase (pfDHFR) from serine to asparagine (S108N) is due to steric interaction between the bulky side chain of N108 and Cl atom of the 5-*p*-Cl aryl group of PYR, which consequently resulted in the reduction in binding affinity between the enzyme and inhibitor. Molecular modeling suggested that the flexible antifolate, such as trimethoprim (TMP) derivatives, could avoid this steric constraint and should be considered as new, potentially effective compounds. The hydrophobic interaction between the side chain of inhibitor and the active site of the enzyme around position 108 was enhanced by the introduction of a longer and more hydrophobic side chain on TMP's 5-benzyl moiety. The prepared compounds, especially those bearing aromatic substituents, exhibited better binding affinities to both wild type and mutant enzymes than the parent compound. Binding affinities of these compounds correlated well with their antimalarial activities against both wild type and resistant parasites. Molecular modeling of the binding of such compounds with pfDHFR also supported the experimental data and clearly showed that aromatic substituents play an important role in enhancing binding affinity. In addition, some compounds with 6-alkyl substituents showed relatively less decrease in binding constants with the mutant enzymes and relatively good antimalarial activities against the parasites bearing the mutant enzymes.

Introduction

Malaria, one of the most widespread tropical diseases, is caused by parasites of *Plasmodium* spp., of which *falciparum* is the most lethal. The emergence of resistant parasites to various available drugs has become a very serious problem in malaria control.[1,2] *Plasmodium falciparum* dihydrofolate reductase (pfDHFR), which is an essential enzyme in the folate pathway and exists as a bifunctional enzyme linked to thymidylate synthase (TS), has long been an important target for malarial therapy. Pyrimethamine (PYR, **1**) and cycloguanil (CYC, **2**), the active metabolite of proguanil, are potent DHFR inhibitors and were effectively used for *P. falciparum* malaria treatment. Unfortunately, resistance of the parasite to these drugs occurred rapidly, and hence, their clinical utility has been drastically affected. The mechanism of resistance has been shown to be due to the various point mutations of DHFR, including those at positions 16, 50, 51, 59, 108, 140, and 164.[3−7]

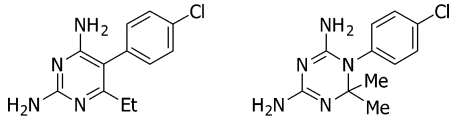

PYR, **1**

CYC, **2**

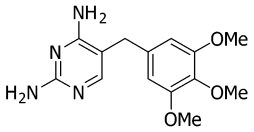

TMP, **3**

During the past few years, molecular modeling of pfDHFR has extensively been studied in order to understand the basis of drug resistance that can lead to the development of new effective inhibitors.[8−11] From a homology model based on leishmania DHFR, McKie et al. pointed out that S108N mutation had led to steric clash with the *p*-Cl atom of PYR.[9] Results from other molecular modeling studies of various different species of DHFRs also gave a similar explanation for the resistance of this mutant.[8,10,11]

It has been suggested that the flexible antifolate could avoid this steric constraint and should be an effective inhibitor.[12] This was demonstrated in the case of WR99210, the triazine derivative with a flexible trichlorophenoxypropyloxy side chain, which is effective against PYR-resistant parasites.[13,14] Trimethoprim (TMP, **3**) also possesses a flexible benzyl side chain, and it was shown that the binding affinity of TMP analogues to mutant enzymes was relatively less affected than PYR, although the relative influence of side chain flexibility must be weighed against other influences of structural changes in the various derivatives.[15] It was also shown that derivatives with a benzyloxy substituent on the 5-benzyl group had favorable binding characteristics.

* To whom correspondence should be addressed. Phone: 662-2015135. Fax: 662-2458332. E-mail: scytr@mahidol.ac.th.
† National Science and Technology Development Agency.
‡ Mahidol University.

10.1021/jm0303352 CCC: $27.50
Published on Web 12/16/2003

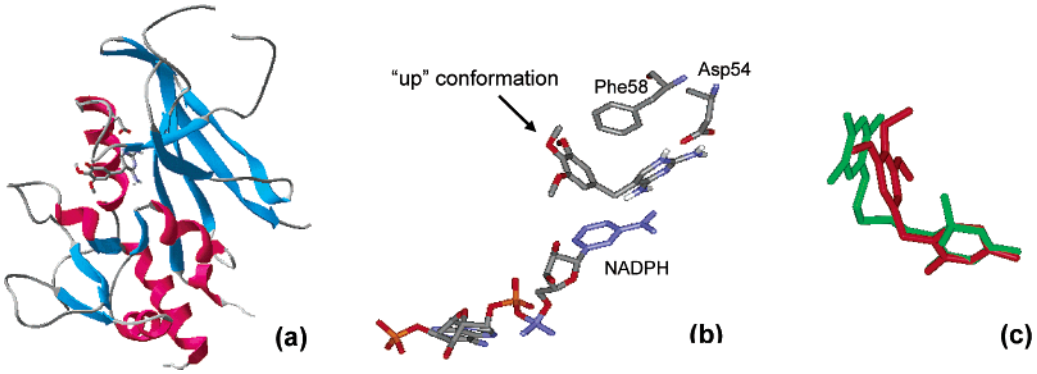

Figure 1. Predicted conformation of TMP in the binding pocket of wild type *P. falciparum* DHFR: (a) overall folding of the enzyme; (b) conformation of TMP with NADPH; (c) superimposition of TMP (red) and WR99210 (green).

Scheme 1

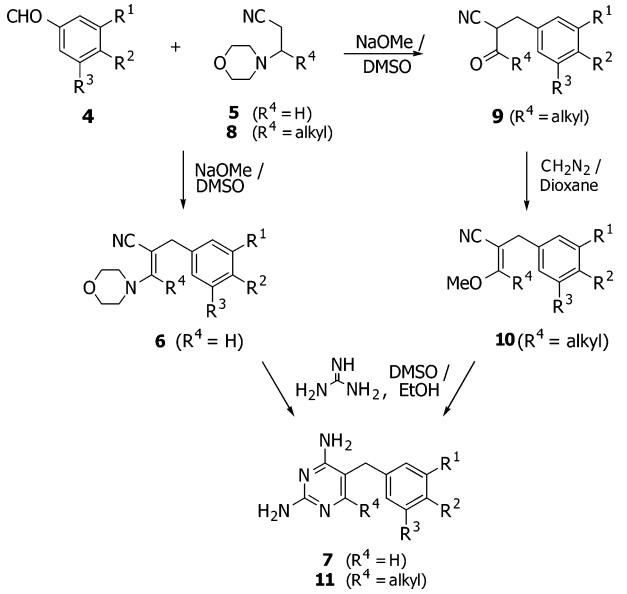

These implied that the aromatic group at the 5-benzyl moiety played an important role in the binding affinity. To explore the significance of aromatic and other hydrophobic substituents on the 5-benzyl moiety, the binding affinity of various TMP derivatives bearing these substituents with both wild type and mutant enzymes was extensively studied. Moreover, molecular modeling of the binding of TMP derivatives with the active site of the recently solved pfDHFR[16] was also studied.

Results and Discussion

Chemical Syntheses. Preparation of TMP analogues was achieved by the improved method recently reported by our group,[15] and the synthetic route is shown in Scheme 1. Derivatives of TMP with the 5-benzyl substituent were synthesized by aldol condensation between 3-morpholinopropionitrile and substituted benzaldehyde, followed by treatment of the intermediates with guanidine. In the cases of derivatives with 6-alkyl substituents, an additional methylation step, using diazomethane, was needed prior to the treatment with guanidine. For derivatives bearing long ether side chains, the preparation of starting aldehydes is outlined in Scheme 2. 4-(3-Hydroxypropoxy)-3-substituted benzaldehyde (**14**) and 3-substituted phenoxy-1-propanol (**17**) were synthesized by alkylation of the corresponding hydroxybenzaldehyde (**12**) or phenol (**16**) with 3-chloro-1-propanol using K_2CO_3/DMF at 80 °C. Treatment of compound **14** with *p*-toluenesulfonyl chloride at 0 °C gave the tosylated product **15** as a white solid. Synthesis of compound **18** was achieved by alkylation of compound **17** with tosylated **15** under NaH/DMF conditions.

Molecular Modeling of pfDHFR Bound with TMP. Since the structures of pfDHFRs were solved during the course of this research, molecular modeling of trimethoprim with the enzyme was conducted with these solved structures in order to understand the mode of binding of the inhibitor in the active site pocket. Predicted conformations of this compound in the active site pocket of wild type and quadruple mutant pfDHFRs are shown in Figures 1 and 2. The benzyl side chain of the inhibitor was found to be oriented in the "up" conformation, bending away from NADPH, as observed in eucaryotes, whereas in bacterial DHFR the benzyl group was pointing "downward" toward the nicotinamide ring.[17,18] In this case, the inhibitor was positioned more closely to NADPH than in the bacteria, and adjustment to the "down" conformation led to steric clash with the nicotinamide ring of NADPH. It is noted

Scheme 2

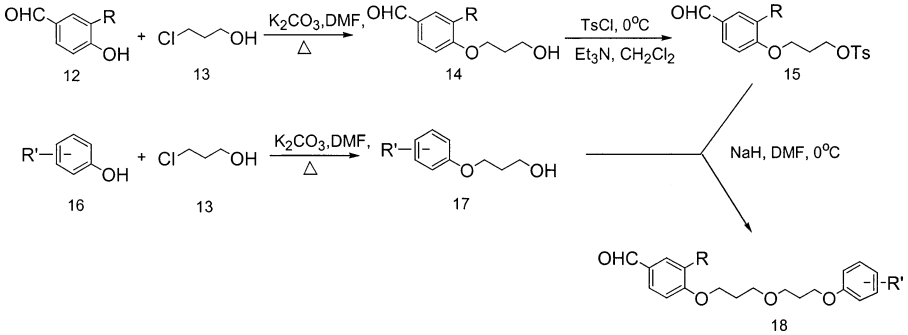

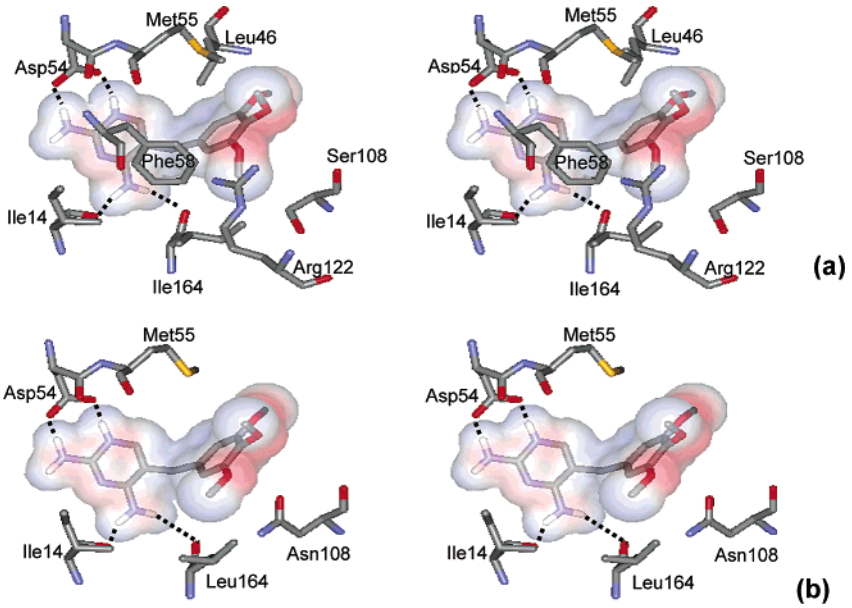

Figure 2. TMP in the binding pocket of pfDHFRs with selected amino acid residues: (a) wild type; (b) quadruple mutant.

that the conformation of TMP in the active site pocket of the enzyme reported in this study is very similar to the established conformation of WR99210 in the same active site (Figure 1c).[16]

As Figures 1a and 2a show, the inhibitor was bound in the active site of the enzyme with its pyrimidine ring occupying the interior of the deep cleft while its benzyl side chain extended toward the entrance of the hydrophobic binding cavity. This inhibitor was held in the pocket by a combination of van der Waals, hydrogen bonding, and ionic interactions with the protein. The key interaction was the hydrogen bonding between carboxylate side chain of Asp54 and both the N1 and 2-amino groups of the pyrimidine ring. Furthermore, the backbone carbonyl oxygens of Ile14 and 164 were located in the plane of the pyrimidine ring, which formed a hydrogen bond with the 4-amino group of the inhibitor. Additional major hydrophobic contacts occurred between the pyrimidine ring and the side chain of Phe58 and Leu46, located above the ring and adjacent to its exterior edge, respectively. Three methoxy groups were in van der Waals contact with the side chain of Met55, Leu46, Ile164, and the nicotinamide ring of NADPH. The model showed that interaction between the side chain of the inhibitor and amino acid at residue 108 and the $\pi-\pi$ interaction caused by the stacking between the phenyl ring of the inhibitor and the nicotinamide ring of NADPH, which took place in case of PYR and CYC,[8,10] were absent and therefore resulted in poor binding. To produce optimal interaction, addition of longer and more hydrophobic substituents was required. However, the space around methoxy group at position 5 was quite limited for modification. Consequently, modification was focused at positions 3 and 4 on the benzyl moiety.

It is shown in Figure 2b that in the case of the quadruple mutant enzyme there is no interaction between the benzyl side chain and the nearby amino acids Met55 and Leu164. In addition, the distance between the backbone oxygen of Leu164 and the 4-amino group of the pyrimidine ring increased significantly, resulting in weaker hydrogen-bonding interaction. All these results are consistent with poor binding of the inhibitor to this mutant enzyme when compared to the results of the wild type.

Inhibition of the Wild Type and Mutant pfDHFRs by TMP Derivatives. From the characteristics of binding discussed, we propose that aromatic and other hydrophobic substituents on the 5-benzyl moiety of TMP would increase the binding affinity, resulting in enhanced enzyme inhibition and parasite killing. The trimethoprim derivatives with these substituents were subjected to screening for inhibitory activity with wild type, S108N, C59RS108N double mutant, C59RS108NI164L triple mutant, and N51IC59RS108NI164L quadruple mutant DHFRs. K_i values for these compounds, binding with wild type and mutant enzymes, are shown in Tables 2−5 along with K_i values of trimethoprim for comparison. Effects of substituents on the inhibitors in their binding to both wild type and mutant DHFRs were assessed by determination of the ratios of inhibition constants for the mutants compared to the wild type enzyme [K_i(mutant)/K_i(wild type)], as well as their K_i values relative to trimethoprim.

The K_i values of trimethoprim analogues having various long-chain alkoxy substituents are shown in Table 2. In the case of compounds **20**−**22**, it was noted that the increase of carbon atoms at the *p*-alkoxy side chain resulted in a decrease of K_i values for both wild type (wt) and mutant enzymes, compared to the simple *p*-methoxy substituent (compound **19**). Binding affinities of derivatives with substituents at positions 3 and 4, compounds **23**−**27**, in which one of these two substituents was a long alkoxy chain, improved the binding by about 5- to 10-fold against both wild type and mutant enzymes. In Table 3, trimethoprim derivatives with aromatic substituents showed relatively more favorable binding to both wild type and mutant enzymes, especially for compound **40**, which is about 30-fold and 60- to 200-fold more effective than trimethoprim against wild type and mutant enzymes, respectively, as has been reported in the previous study.[15] In addition, the change from H to an alkoxy group at the meta position improved binding affinity to both wild type and mutant enzymes (e.g., compounds **38**−**41**) while the K_i values

Table 1. Data of TMP Analogues

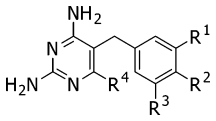

compd	R^1	R^2	R^3	R^4	yield (%)	mp (°C)	formula	*m/z*: $[M + 1]^+$	anal.
19	H	OMe	H	H	68	206.5−207.5	$C_{12}H_{14}N_4O$	231.1221	CHN
20	H	OPr^n	H	H	74	164−165	$C_{14}H_{18}N_4O$	259.1569	CHN
21	H	$OPen^n$	H	H	65	165−166	$C_{16}H_{22}N_4O$	287.1867	CHN
22	H	$OHep^n$	H	H	68	161.5−162.5	$C_{18}H_{26}N_4O$	315.2184	CHN
23	OPr^n	OMe	H	H	63	151−152	$C_{15}H_{20}N_4O_2$	289.1656	HN[b]
24	OBu^n	OMe	H	H	65	153.5−154.5	$C_{16}H_{22}N_4O_2$	303.1826	CH[c]
25	$OPen^n$	OMe	H	H	71	161−162	$C_{17}H_{24}N_4O_2$	317.1980	CHN
26	$OHep^n$	OMe	H	H	77	138.5−139.5	$C_{19}H_{28}N_4O_2$	345.2297	CHN
27	OEt	$OPen^n$	H	H	74	151.5−152	$C_{18}H_{26}N_4O_2$	331.2136	CHN
28	OMe	OEt	H	H	65	194.5−195.5	$C_{14}H_{18}N_4O_2$	275.1520	CHN
29	OMe	OMe	H	H	85	234.5−235	$C_{13}H_{16}N_4O_2$	261.1349	CHN
30[a]	OMe	OCH_2Ph	H	H	84	162.5−163	$C_{19}H_{20}N_4O_2$	337.1672	CHN
31[a]	OEt	OCH_2Ph	H	H	65	173.5−174	$C_{20}H_{22}N_4O_2$	351.1828	CHN
32[a]	OCH_2Ph	OCH_2Ph	H	H	63	137−137.5	$C_{25}H_{24}N_4O_2$	413.1983	CHN
33	H	OCH_2Ph	H	H	67	201.5−202	$C_{18}H_{18}N_4O$	307.1569	CHN
34	OCH_2Ph	H	H	H	76	154−155	$C_{18}H_{18}N_4O$	307.1562	CHN
35	OPh	H	H	H	79	202−203	$C_{17}H_{16}N_4O$	293.1408	CHN
36	OCH_2Ph	OMe	H	H	89	214.5−215.5	$C_{19}H_{20}N_4O_2$	337.1665	CHN
37[a]	H	OCH_2-[3,4,5-$(OMe)_3$]Ph	H	H	89	174−174.5	$C_{21}H_{24}N_4O_4$	397.1905	CHN
38[a]	OMe	OCH_2-[3,4,5-$(OMe)_3$]Ph	H	H	90	155.5−156	$C_{22}H_{26}N_4O_5$	427.1985	CHN
39[a]	OEt	OCH_2-[3,4,5-$(OMe)_3$]Ph	H	H	83	153−154	$C_{23}H_{28}N_4O_5$	441.2133	CHN
40[a]	OPr^n	OCH_2-[3,4,5-$(OMe)_3$]Ph	H	H	65	143.5−144.5	$C_{24}H_{30}N_4O_5$	455.2296	CHN
41[a]	OBu^n	OCH_2-[3,4,5-$(OMe)_3$]Ph	H	H	87	154.5−155.5	$C_{25}H_{32}N_4O_5$	469.2447	CHN
42	H	OC_3H_6Ph	H	H	85	167−168	$C_{23}H_{28}N_4O_5$	335.1870	CHN
43[a]	OMe	OC_3H_6Ph	H	H	80	134.5−135.5	$C_{21}H_{24}N_4O_2$	365.1975	CHN
44	OEt	OC_3H_6Ph	H	H	87	137−138	$C_{22}H_{26}N_4O_2$	379.2135	CHN
45	H	OC_3H_6OPh	H	H	83	151.5−152	$C_{20}H_{22}N_4O_2$	351.1823	CHN
46	OMe	OC_3H_6OPh	H	H	77	154−154.5	$C_{21}H_{24}N_4O_3$	381.1931	CHN
47	OEt	OC_3H_6OPh	H	H	84	141.5−142	$C_{22}H_{26}N_4O_3$	395.2084	CHN
48	H	$OC_3H_6OC_3H_6OPh$	H	H	66	108.5−109	$C_{23}H_{28}N_4O_3$	409.2240	CH[d]
49	OMe	$OC_3H_6OC_3H_6OPh$	H	H	65	131.2−131.8	$C_{24}H_{30}N_4O_4$	439.2345	CHN
50	OEt	$OC_3H_6OC_3H_6OPh$	H	H	68	147.5−148	$C_{25}H_{32}N_4O_4$	453.2506	CHN
51	OMe	OMe	OMe	Me	89	193−194	$C_{15}H_{20}N_4O_3$	305.1612	CHN
52	OMe	OMe	OMe	Et	90	218.219	$C_{16}H_{22}N_4O_3$	319.1769	CHN
53	OMe	OCH_2Ph	H	Me	91	180−181	$C_{20}H_{22}N_4O_2$	351.1816	HN[e]
54	OMe	OCH_2Ph	H	Et	87	176−177	$C_{21}H_{24}N_4O_2$	365.1970	CHN
55[a]	OCH_2Ph	OCH_2Ph	H	Me	92	153−153.5	$C_{26}H_{26}N_4O_2$	427.2130	CHN
56[a]	OCH_2Ph	OCH_2Ph	H	Et	91	114.5−115	$C_{27}H_{28}N_4O_2$	441.2290	CHN
57	OPr^n	OCH_2-[3,4,5-$(OMe)_3$]Ph	H	Et	89	161−162	$C_{26}H_{34}N_4O_5$	483.2650	HN[f]

[a] Data from ref 13. [b] C: calcd, 62.46; found, 61.76. [c] N: calcd, 18.54; found, 19.20. [d] N: calcd, 13.72; found, 14.59. [e] C: calcd, 68.55; found, 67.82. [f] C: calcd, 64.69; found, 63.85.

Table 2. K_i Values of Trimethoprim Derivatives with Various Long Alkoxy Chain Substituents

compd	K_i wt (nM)	rel to TMP	K_i C59RS108N (nM)	rel to TMP	K_i C59RS108NI164L (nM)	rel to TMP	K_i N51I C59RS108NI164L (nM)	rel to TMP
TMP	10.3 ± 0.5	1.0	242.1 ± 40.1	1.0	5688.7 ± 557.1	1.0	6664.5 ± 1516.3	1.0
19	23.5 ± 8.0	2.3	464.1 ± 59.1	1.9	3957.8 ± 1358.4	0.7	20491.0 ± 5209.4	3.1
20	15.1 ± 1.5	1.5	211.5 ± 31.5	0.9	1091.3 ± 171.0	0.2	1518.0 ± 268.2	0.2
21	8.6 ± 0.6	0.8	137.3 ± 18.5	0.6	539.5 ± 103.3	0.1	914.6 ± 147.4	0.1
22	17.8 ± 0.5	1.7	196.3 ± 25.1	0.8	2208.4 ± 229.0	0.4	1380.0 ± 190.8	0.2
23	1.8 ± 0.1	0.2	52.1 ± 10.0	0.2	144.4 ± 22.2	0.03	919.6 ± 176.8	0.1
24	2.5 ± 0.2	0.2	194.1 ± 24.9	0.8	771.8 ± 106.9	0.1	1033.3 ± 48.3	0.2
25	2.2 ± 0.2	0.2	134.5 ± 18.5	0.5	252.6 ± 1.0	0.04	444.2 ± 71.9	0.1
26	3.1 ± 0.1	0.3	103.5 ± 8.2	0.4	292.4 ± 64.4	0.05	445.1 ± 67.2	0.1
27	1.6 ± 0.3	0.1	46.6 ± 5.7	0.2	1162.5 ± 638.1	0.2	901.7 ± 225.5	0.1
28	15.4 ± 0.8	1.5	187.4 ± 20.6	0.8	3541.8 ± 1788.8	0.6	11817.9 ± 950.6	1.8
29	11.5 ± 0.6	1.1	234.8 ± 32.6	1.0	2646.8 ± 460.3	0.5	13858.0 ± 970.7	2.1

decreased when the methoxy group (e.g., compounds **30** and **38**) at this position was replaced by an ethoxy functionality (e.g., compounds **31** and **39**). These results support our hypothesis concerning the addition of more hydrophobic substituents to produce the optimal interaction and the importance of the aromatic ring on the binding affinity.

An attempt to extend the aromatic side chain (Table 4) by increasing the number of carbon atoms of the alkyl (compounds **42**−**44**) or ether chain (compounds **45**−**50**) had no significant effect on the binding affinity with the enzymes, compared to derivatives having aromatic substituents without any extension as shown in Table 3. Derivatization at the 6-position of the pyrimidine ring by replacing an H atom with either a methyl or an ethyl group did not improve the binding affinity to wild type enzyme (Table 5) compared to those without the 6-alkyl substituent (Table 3). However, in the case of compound

Table 3. K_i Values of Trimethoprim Derivatives with Various Aromatic Substituents

compd	K_i wt (nM)	rel to TMP	K_i C59RS108N (nM)	rel to TMP	K_i C59RS108NI164L (nM)	rel to TMP	K_i N51I C59RS108NI164L (nM)	rel to TMP
30	2.2 ± 0.5	0.2	60.7 ± 8.7	0.3	1974.1 ± 123.3	0.4	1375.7 ± 223.4	0.21
31	0.8 ± 0.3	0.09	9.7 ± 1.4	0.04	570.3 ± 70.1	0.1	431.4 ± 112.4	0.06
32	1.7 ± 0.2	0.2	60.2 ± 2.6	0.2	491.2 ± 56.0	0.09	2454. ± 257.1	0.4
33	6.5 ± 0.5	0.6	101.0 ± 22.8	0.4	994.0 ± 289.2	0.2	4636.7 ± 730.8	0.7
34	6.3 ± 0.6	0.6	113.5 ± 17.6	0.9	515.4 ± 127.8	0.09	455.5 ± 124.8	0.07
35	5.3 ± 0.5	0.5	81.7 ± 16.9	0.3	161.2 ± 16.2	0.03	671.4 ± 281.9	0.1
36	7.2 ± 0.9	0.7	143.4 ± 17.8	0.6	629.8 ± 56.9	0.11	1129.6 ± 55.7	0.2
37	1.3 ± 0.2	0.1	5.2 ± 0.3	0.02	511.9 ± 62.9	0.09	76.5 ± 20.2	0.01
38	0.6 ± 0.0	0.06	8.7 ± 1.0	0.04	47.6 ± 5.4	0.01	124.0 ± 12.9	0.02
39	0.3 ± 0.0	0.03	2.2 ± 0.1	0.009	24.7 ± 2.6	0.004	119.3 ± 22.5	0.02
40	0.4 ± 0.2	0.04	3.5 ± 0.8	0.001	88.6 ± 6.2	0.02	35.8 ± 3.6	0.005
41	0.4 ± 0.2	0.04	5.6 ± 0.4	0.02	105.6 ± 8.4	0.02	258.6 ± 39.3	0.04

Table 4. K_i Values of Trimethoprim Derivatives with Various Long-Chain Aromatic and Ether Substituents

compd	K_i wt (nM)	rel to TMP	K_i C59RS108N (nM)	rel to TMP	K_i C59RS108NI164L (nM)	rel to TMP	K_i N51I C59RS108NI164L (nM)	rel to TMP
42	5.9 ± 1.1	0.57	58.1 ± 17.0	0.44	3044.8 ± 595.7	0.54	801.4 ± 210.4	0.12
43	1.8 ± 0.4	0.17	44.2 ± 2.7	0.33	3100.2 ± 456.9	0.54	1122.8 ± 644.8	0.17
44	1.0 ± 0.3	0.10	10.6 ± 1.2	0.08	374.1 ± 21.8	0.06	525.3 ± 148.3	0.08
45	6.5 ± 1.5	0.63	169.9 ± 11.4	0.70	470.6 ± 28.4	0.08	2261.0	0.34
46	2.0 ± 0.6	0.19	37.1 ± 0.8	0.15	256.9 ± 30.6	0.05	605.8 ± 38.1	0.09
47	0.6 ± 0.2	0.06	47.7 ± 6.5	0.2	166.4 ± 7.1	0.03	770.1	0.12
48	7.0 ± 0.5	0.68	107.7 ± 11.6	0.45	263.6 ± 16.0	0.05	1589.0 ± 33.5	0.24
49	1.8 ± 0.3	0.18	153.5 ± 22.9	0.63	424.8 ± 21.9	0.07	2191.7	0.33
50	2.3 ± 0.4	0.22	46.9 ± 2.2	0.19	313.7 ± 68.8	0.06	937.4 ± 49.9	0.14

Table 5. K_i Values of Trimethoprim Derivatives with Various 6-Alkyl Substituents

compd	K_i wt (nM)	rel to TMP	K_i C59RS108N (nM)	rel to TMP	K_i C59RS108NI164L (nM)	rel to TMP	K_i N51I C59RS108NI164L (nM)	rel to TMP
51	38.2 ± 3.1	3.7	520.3 ± 122.8	2.2	1364.3 ± 132.1	0.24	1634.3 ± 362.6	0.25
52	4.3 ± 0.6	0.4	116.4 ± 25.9	0.5	466.8 ± 37.7	0.08	697.6 ± 41.1	0.11
53	3.4 ± 0.5	0.3	89.5 ± 12.7	0.4	66.3 ± 14.9	0.01	93.4 ± 2.6	0.01
54	3.5 ± 0.5	0.3	60.1 ± 8.1	0.25	3737.7 ± 1497.3	0.66	732.5 ± 98.1	0.11
55	8.6 ± 0.4	0.8	80.0 ± 10.3	0.3	174.6 ± 24.1	0.03	241.0 ± 36.6	0.04
56	3.7 ± 0.9	0.4	99.1 ± 17.2	0.4	273.4 ± 24.7	0.05	204.7 ± 42.5	0.03
57	1.8 ± 1.0	0.17	48.7 ± 6.95	0.20	154.2 ± 42.0	0.03	693.1 ± 125.6	0.1

52, small decreases in K_i values were observed (compared to TMP). These results might be due to steric clash of the larger substituent with the benzyl group, resulting in conformational change that affected the binding affinity to the enzyme. Some of these compounds (i.e., **51**−**56**) showed better binding affinity, specifically with the mutant enzymes. The results described above implied that the alkyl group at position 6 on the pyrimidine ring played a significant role in the binding affinity with mutant enzymes.

In Vitro Antiplasmodial Activity. All compounds were also subjected to an in vitro malaria screening system against wild type and resistant *Plasmodium falciparum* parasites carrying various mutation enzymes, and some of these results are shown in Table 6.

Antiplasmodial activity (IC_{50} values) of compounds described in this study ranged in the micromolar regions. Although not as good as predicted according to the enzyme inhibition constants, some exhibited IC_{50} values against both wild type and resistant parasites at low micromolar levels (e.g., compounds **37**−**41**). Correlations between antimalarial and inhibitory activities of these analogues are shown in Figure 3, where values of log K_i (of wild type, double, triple, and quadruple mutant enzymes) are plotted against the corresponding log IC_{50}. Antimalarial activity of almost all compounds against wild type and resistant strains correlated linearly with the ability of these compounds to inhibit wild type and mutant DHFRs. This implied that the drug target in the cell was the enzyme DHFRs. However, lack of correlation between antimalarial and inhibitory activities of some trimethoprim analogues was also observed. For example, compounds **33**−**36** showed better K_i values than TMP for wild type enzyme but exhibited less potency in antimalarial activity against wild type parasite. The discrepancies from the expected correlation between the K_i values and the antimalarial activities can be due to various reasons, including differences in drug transport into and out of the parasite, access of the drug to the target enzyme, and the presence of competing sites for drug binding.

Toxicity tests of these compounds to evaluate the selective inhibition against three mammalian cell lines, African green monkey kidney fibroblast (Vero cells), human epidermoid carcinoma (KB), and human breast cancer (BC), showed that the compounds are relatively nontoxic compared to their activity against the malaria parasites (see data in Supporting Information).

Molecular Modeling of Binding of Trimethoprim Derivatives with pfDHFR. To understand further the role of hydrophobic and aromatic substituents on the binding affinity, the molecular modeling of compound **40** (which showed high binding affinity to both wild type and mutant enzymes) bound with both wild type and quadruple mutant enzymes was studied. Predicted conformations of this compound in the active site pocket

Table 6. Antimalarial Activity of Some of Trimethoprim Derivatives, IC_{50} (μM)

compd	TM4/8.2[a]	rel to TMP	K1CB1[b]	rel to TMP	Csl-2[c]	rel to TMP	Vl/S[d]	rel to TMP
30	4.66 ± 1.71	0.70	>100[e]	>0.73	25.61 ± 1.26	0.21	38.02 ± 1.69	<0.19
31	0.47 ± 0.10	0.07	16.59 ± 1.85	0.12	14.36 ± 2.90	0.12	16.47 ± 4.63	<0.08
32	3.12 ± 0.56	0.47	14.58 ± 2.33	0.11	6.75 ± 4.28	0.06	8.13 ± 1.53	<0.04
33	15.15 ± 5.10	2.27	17.14 ± 6.56	0.13	15.26 ± 2.35	0.13	21.49 ± 2.25	<0.11
34	15.22 ± 5.42	2.28	3.52 ± 0.82	0.03	3.33 ± 0.19	0.03	12.75 ± 3.18	<0.06
35	19.08 ± 5.98	2.86	3.69 ± 0.51	0.03	3.517 ± 1.01	0.03	29.61 ± 20.21	<0.15
36	17.48 ± 0.74	2.62	3.83 ± 0.45	0.03	5.73 ± 1.94	0.05	>50[e]	0.25
37	0.68 ± 0.21	0.10	19.88 ± 3.79	0.15	19.85 ± 7.49	0.17	21.12 ± 0.09	<0.11
38	0.31 ± 0.06	0.05	27.76 ± 10.63	0.13	30.58 ± 7.47	0.26	26.08 ± 2.30	<0.13
39	0.07 ± 0.02	0.01	5.01 ± 1.53	0.04	13.15 ± 0.73	0.11	19.45 ± 0.19	<0.10
40	0.15 ± 0.05	0.02	4.29 ± 0.96	0.03	7.70 ± 4.34	0.06	9.75 ± 0.92	<0.05
41	0.33 ± 0.06	0.05	10.16 ± 4.23	0.07	3.40 ± 0.33	0.03	15.91 ± 5.68	<0.13
51	22.73 ± 2.77	3.41	>100[e]	>0.73	90.81 ± 2.28	0.76	>100[e]	0.5
52	2.40 ± 0.67	0.36	>50[e]	>0.37	>50[e]	>0.42	>50[e]	0.25
53	6.84 ± 1.36	1.03	25.24 ± 7.02	0.18	2.85 ± 0.40	0.02	4.82 ± 1.87	<0.02
54	5.06 ± 1.45	0.76	16.26 ± 3.71	0.12	5.37 ± 1.78	0.05	11.30 ± 0.82	<0.06
55	4.48 ± 0.29	0.67	4.38 ± 1.69	0.03	2.64 ± 0.91	0.02	3.11 ± 0.30	<0.02
56	3.57 ± 0.52	0.54	4.18 ± 1.47	0.03	3.46 ± 0.51	0.03	3.02 ± 0.29	<0.02

[a] Parasite strain with wild type DHFR. [b] Parasite strain with double mutation (C59R + S108N) DHFR. [c] Parasite strain with triple mutation (C59R + S108N + I164L) DHFR. [d] Parasite strain with quadruple mutation (N51I + C59R + S108N + I164L) DHFR. [e] Maximun concentration that the inhibitor could be dissolved in DMSO.

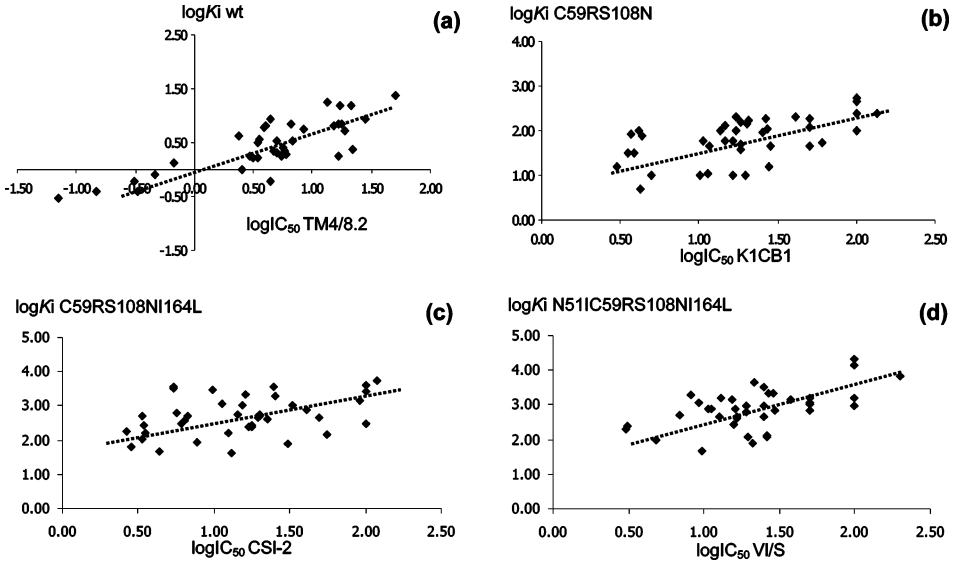

Figure 3. Correlation between (a) log K_i wt and IC_{50} TM4/8.2, (b) log K_i C59RS108N and IC_{50} K1CB1, (c) log K_i C59RS108NI164L and IC_{50} Csl-2, (d) log K_i N51IC59RS108NI164L and IC_{50} Vl/S.

of wild type and quadruple mutant DHFRs are shown in Figure 4.

In Figure 4a, the model showed that the aromatic substituent of this inhibitor was stacked against the phenyl side chain of Phe116 and formed a $\pi-\pi$ interaction. This interaction led to better binding affinity of trimethoprim derivatives having aromatic substituents to both wild type and mutant enzymes than the derivatives with alkoxy substituents. The additional three methoxy groups on the benzyl substituent were in van der Waals contact with the amino acid residues Pro113, Phe116, Cys50, and Met55 near the entrance of the active site. The *p*-methoxy oxygen was positioned 3.27 Å from the side chain of Cys50 and could have H-bonding interaction. Although well-documented hydrogen bonds involving methoxy groups were rare, they were not entirely unknown.[19] Moreover, the propoxy group at the 3′-position was bound closely to the side chain of Ile112, Val45, and Leu46 with the distances of 3.75, 3.54, and 3.55 Å, respectively, close enough to be involved in van der Waals interactions. This model supported the experimental data, which showed very good binding to both wild type and mutant enzymes. For the quadruple mutant enzyme (Figure 4b), the solved structure[16] showed significant movement of residues 48−51 and 164−166, which opened up the gap between residues 50 and 164 in the active site. Accordingly, the distance between the inhibitor and the nearby amino acid side chains in this mutant enzyme was larger than that observed in wild type enzyme. This leads to a decrease in various interactions, for example, H-bonding between the side chain of Cys50 and *p*-methoxy oxygen of the benzyl substituent, van der Waals interaction of Met55 and the methoxy group, favorable stacking between the aromatic ring and the phenyl side chain of Phe116, and H-bonding between the backbone oxygen of Leu164 and the 4-amino group of the pyrimidine ring, which resulted in a reduction of binding affinity between the inhibitor and the enzyme.

Compounds with 6-alkyl substituents (**52**−**56**) showed relatively less decrease in binding affinities with the mutant enzymes and are therefore of higher potential interest. To study the effect of the alkyl group at the 6-position of the pyrimidine ring on the binding affinity,

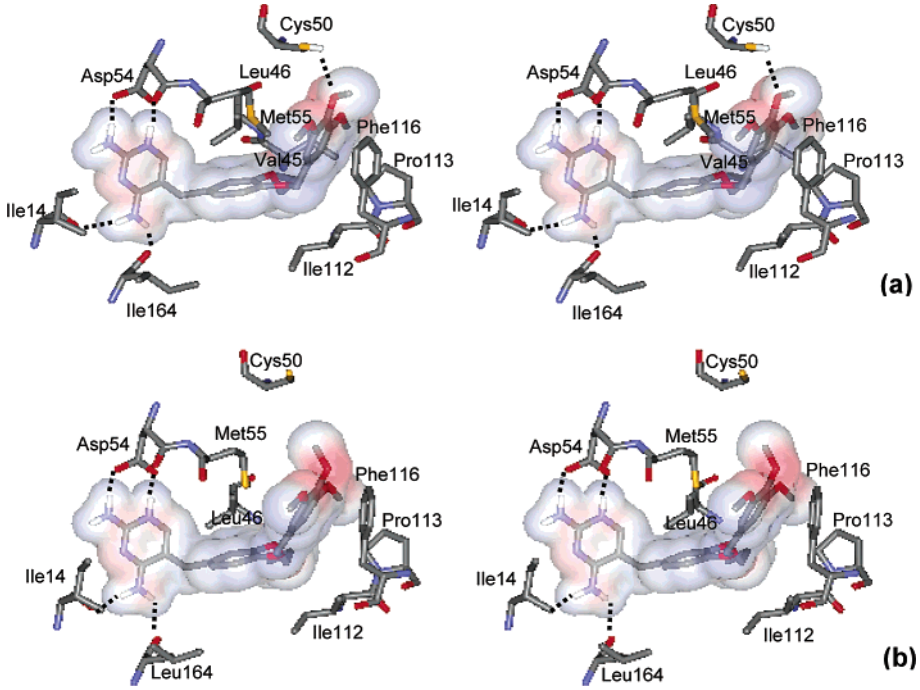

Figure 4. Compound **40** in the binding pocket of pfDHFR with selected amino acid residues: (a) wild type; (b) quadruple mutant.

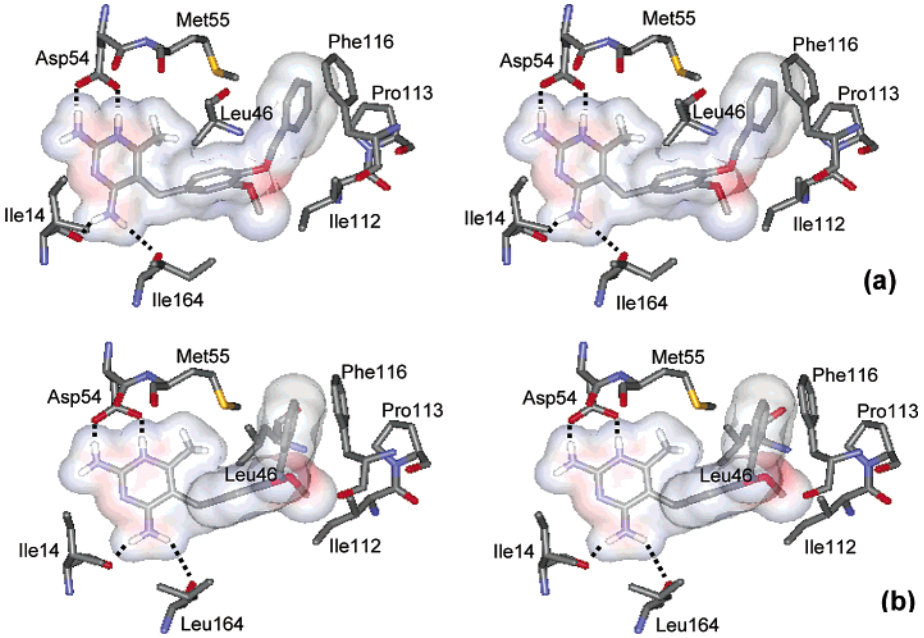

Figure 5. Compound **53** in the binding pocket of pfDHFR with selected amino acid residues: (a) wild type; (b) quadruple mutant.

molecular modeling of compound **53** bound to both wild type and quadruple mutant enzymes was performed, and results are shown in Figure 5. Because of the steric interaction between the alkyl group at the 6-position and the 5-benzyl group, the conformation of the 5-benzyl moiety was adjusted in order to avoid this steric constraint and also the aromatic substituent was repositioned. This phenomenon led to unfavorable stacking interaction between the aromatic substituent and the phenyl side chain of Phe116 of the wild type enzyme, resulting in the reduction of binding affinity of this inhibitor to the enzyme compared with those without 6-alkyl substituents (compound **30**). For quadruple mutant enzyme (Figure 5b), there is relatively more favorable stacking interaction between aromatic substituent and the phenyl side chain of Phe116 after the conformation adjustment of the 5-benzyl moiety. Moreover, the additional methyl group at position 6 on the pyrimidine ring was in van der Waals contact with Leu46 and Met55. All these interactions led to better binding affinity of this inhibitor to the mutant enzymes.

Conclusion

The extension of the hydrophobic side chain on the 5-benzyl moiety of 5-benzyl-2,4-diaminopyrimidine led to better binding affinity to both wild type and mutant enzymes than that of trimethoprim, especially with benzyloxy substituents that were about 5- to 30-fold and 60- to 200-fold more effective against wild type and mutant enzymes, respectively. Some compounds (**52**–**56**) showed relatively less decrease in binding affinities with the mutant enzymes and higher antimalarial

activities and are therefore of higher potential interest. These compounds also exhibited IC_{50} values against wild type and resistant parasites at low micromolar levels, which correlated well with their binding affinity. Molecular modeling studies of pfDHFR bound with trimethoprim derivatives bearing aromatic substituents showed the stacking of the aromatic substituent with the phenyl side chain of Phe116. Evidently, this interaction led to better binding affinity to both wild type and mutant enzymes than those derivatives bearing alkoxy substituents.

Experimental Section

Methods and Materials. For the synthesis of TMP analogues, solvents (DMSO, ethanol, and dioxane) were dried according to standard methods. Reagents were purchased from Fluka, Merck, and Sigma-Aldrich Ltd. and were distilled before use. For enzyme studies, chemicals were obtained from Sigma-Aldrich Ltd., Merck, and BDH and were used without further purification. Melting points were determined by an Electrothermal 9100 melting point apparatus and were uncorrected. Nuclear magnetic resonance (NMR) spectra were recorded in DMSO-d_6 and $CDCl_3$ on a Bruker DRX 400 spectrometer; chemical shifts are reported in parts per million (ppm) using TMS (0 ppm) as the internal standard. Mass spectra were recorded on a Micromass LCT using the electrospray ionization technique. Elemental analyses were carried out using a Perkin-Elmer elemental analyzer 2400.

Chemical Syntheses of TMP Analogues. TMP analogues were synthesized by an improved method described in a previous study,[15] as shown in Scheme 1, and the results are summarized in Table 1. The general procedure for the syntheses of long-chain ether-substitued benzaldehyde is outlined in Scheme 2.

Preparation of Compound 14. To a suspension of K_2CO_3 (15.2 g, 0.11 mol) in DMF (10 mL) was added a solution of 3-substitued 4-hydroxybenzaldehyde (**12**, 0.1 mol) in DMF (10 mL). After the reaction mixture was heated at 60 °C for 30 min, a solution of 3-chloro-1-propanol (**13**, 9.2 g, 0.11 mol) in DMF (5 mL) was added dropwise and the mixture was left stirring at 60 °C overnight. The mixture was neutralized with diluted aqueous HCl and then extracted with CH_2Cl_2, dried over $MgSO_4$, and evaporated to dryness under reduced pressure to yield the crude product as a yellow oil. The crude product was purified by column chromatography (silica gel, 55% EtOAc/45% hexane as developing solvent) to obtain the desired product as a colorless oil.

4-(3-Hydroxypropoxy)benzaldehyde (14a, R = H): colorless oil (13.7 g, 76%); ^{1}H NMR (400 MHz, $CDCl_3$) δ 2.02 (2H, quint, J = 6.1 Hz, $CH_2CH_2CH_2$), 3.06 (1H, s, OH), 3.81 (2H, t, J = 6.1 Hz, $HOCH_2CH_2$), 4.13 (2H, t, J = 6.1 Hz, $ArOCH_2CH_2$), 6.94 (2H, d, J = 8.6 Hz, ArH), 7.74 (2H, d, J = 8.6 Hz, ArH), 9.78 (1H, s, CHO).

3-Methoxy-4-(3-hydroxypropoxy)benzaldehyde (14b, R = OMe): colorless oil (17.0 g, 81%); ^{1}H NMR (400 MHz, $CDCl_3$) δ 2.15 (2H, tt, J = 6.0, 4.9 Hz, $CH_2CH_2CH_2$), 2.40 (1H, bs, OH), 3.91 (2H, t, J = 4.9 Hz, $HOCH_2CH_2$), 3.94 (3H, s, OCH_3), 4.30 (2H, t, J = 6.0 Hz, $ArOCH_2CH_2$), 7.01 (1H, d, J = 8.0 Hz, ArH), 7.43 (1H, s, ArH), 7.47 (1H, d, J = 8.0 Hz, ArH), 9.87 (1H, s, CHO).

3-Ethoxy-4-(3-hydroxypropoxy)benzaldehyde (14c, R = OEt): colorless oil (16.1 g, 72%); ^{1}H NMR (400 MHz, $CDCl_3$) δ 1.47 (3H, t, J = 7.0 Hz, OCH_2CH_3), 2.14 (2H, quint, J = 5.6 Hz, $CH_2CH_2CH_2$), 2.730 (1H, t, J = 5.7 Hz, CH_2OH), 3.91 (2H, dt, J = 5.6, 5.6 Hz, $HOCH_2CH_2$), 4.21 (2H, q, J = 7.0 Hz, OCH_2CH_3), 4.29 (2H, t, J = 5.7 Hz, $ArOCH_2CH_2$), 6.99 (1H, d, J = 8.1 Hz, ArH), 7.40 (1H, d, J = 1.6 Hz, ArH), 7.44 (1H, dd, J = 8.1, 1.6 Hz, ArH), 9.85 (1H, s, CHO).

Preparation of Compound 15. To a solution of compound **14** (0.05 mol) in CH_2Cl_2 (5 mL) and Et_3N (9 mL) was added *p*-toluenesulfonyl chloride (14.3 g, 0.075 mol) at 0 °C, and the reaction mixture was continuously stirred for 2 h. After neutralization with diluted aqueous HCl, the reaction mixture was extracted with CH_2Cl_2, dried over $MgSO_4$, and evaporated to dryness. Purification by column chromatography (silica gel, 25% EtOAc/45% hexane as eluent) gave compound **15** as a white solid. NMR spectra of compounds **15a**−**c** indicated that they were of high purity; therefore, compounds **15a**−**c** were used in the next step without further purification.

4-[3-(4-Toluenesulfonyl)propoxy]benzaldehyde (15a, R = H): white solid (10.4 g, 62%); ^{1}H NMR (400 MHz, $CDCl_3$) δ 2.17 (2H, quint, J = 5.4 Hz, $CH_2CH_2CH_2$), 2.37 (3H, s, $ArCH_3$), 4.06 (2H, t, J = 5.4 Hz, $ArOCH_2CH_2$), 4.26 (2H, t, J = 5.4 Hz, $CH_2CH_2OSO_2$), 6.88 (2H, d, J = 8.3 Hz, ArH), 7.25 (2H, d, J = 7.8 Hz, ArH), 7.76 (2H, d, J = 7.8 Hz, ArH), 7.81 (2H, d, J = 8.3 Hz, ArH), 9.90 (1H, s, CHO).

3-Methoxy-4-[3-(4-toluenesulfonyl)propoxy]benzaldehyde (15b, R = OMe): white solid (10.7 g, 59%); ^{1}H NMR (400 MHz, $CDCl_3$) δ 2.23 (2H, tt, J = 5.9, 6.0 Hz, $CH_2CH_2CH_2$), 2.38 (3H, s, $ArCH_3$), 3.88 (3H, s, OCH_3), 4.18 (2H, t, J = 6.0 Hz, $ArOCH_2CH_2$), 4.30 (2H, t, J = 5.9 Hz, $CH_2CH_2OSO_2$), 6.89 (1H, d, J = 8.1 Hz, ArH), 7.25 (2H, d, J = 8.1 Hz, ArH), 7.40 (1H, d, J = 1.3 Hz, ArH), 7.43 (1H, dd, J = 8.1, 1.3 Hz, ArH), 7.77 (2H, d, J = 8.1 Hz, ArH), 9.87(1H, s, CHO).

3-Ethoxy-4-[3-(4-toluenesulfonyl)propoxy]benzaldehyde (15c, R = OEt): white solid (12.5 g, 66%); ^{1}H NMR (400 MHz, $CDCl_3$) δ 1.42 (3H, t,J = 6.9 Hz, CH_2CH_3), 2.21 (2H, quint, J = 5.9 Hz, $CH_2CH_2CH_2$), 2.37 (3H, s, CH_3), 4.08 (4H, m, $ArOCH_2CH_2$, $ArOCH_2CH_3$), 4.29 (2H, t, J = 5.9 Hz, $CH_2CH_2OSO_2$), 6.87 (1H, d, J = 8.1 Hz, ArH), 7.23 (2H, d, J = 8.1 Hz, ArH), 7.37 (1H, s, ArH), 7.39 (1H, d, J = 8.1 Hz, ArH), 7.75 (2H, d, J = 8.1 Hz, ArH), 9.85 (1H, s, CHO).

Preparation of Compound 17. Compound **17** was prepared from substituted phenol (**16**) and chloropropanol (**13**) according to the procedure described for the synthesis of compound **14** and was purified by column chromatography (silica gel, 60% EtOAc/40% hexane as eluent). Compounds **17a** and **17b** were of high purity (NMR spectra); therefore, they were used in the next reaction step without additional purification.

3-Phenoxy-1-propanol (17a, R′ = H): colorless oil (10.5 g, 69%); ^{1}H NMR (400 MHz, $CDCl_3$) δ 2.03 (2H, tt, J = 6.1, 6.2, Hz, $CH_2CH_2CH_2$), 3.61 (1H, bs, OH), 3.82 (2H, t, J = 6.2 Hz, CH_2CH_2OH), 4.07 (2H, t, J = 6.1 Hz, $ArOCH_2CH_2$), 6.97 (3H, m, ArH), 7.32 (2H, m, ArH).

3-(2,4,5-Trichlorophenoxy)-1-propanol (17b, R′ = 2,4,5-trichloro): colorless oil (18.4 g, 72%); ^{1}H NMR (400 MHz, $CDCl_3$) δ 2.09 (2H, tt, J = 6.0, 5.8, Hz, $CH_2CH_2CH_2$), 2.42 (1H, bs, OH), 3.88 (2H, t, J = 5.8 Hz, CH_2CH_2OH), 4.15 (2H, t, J = 6.0 Hz, $ArOCH_2CH_2$), 7.0 (1H, d, J = 4.6 Hz, ArH), 7.42 (1H, d, J = 4.6 Hz, ArH).

Preparation of Compound 18. To a suspension of NaH (0.92 g, 21 mmol) in DMF (2 mL) at 0 °C was added a solution of alcohol **17** (20 mmol) in DMF (3 mL), and the reaction mixture was left stirring at 0 °C for 30 min. Then a solution of aldehyde **15** (21 mmol) in DMF (5 mL) was added. After continuous stirring at 0 °C for 2 h, the reaction mixture was carefully neutralized with diluted aqueous HCl solution, extracted with CH_2Cl_2, dried over $MgSO_4$, and evaporated to dryness. Purification by column chromatography (silica gel, 40% EtOAc/75% hexane as eluent) gave pure compound **18** as a colorless oil.

4-[3-(3-Phenoxypropoxy)propoxy]benzaldehyde (18a, R = R′ = H): colorless oil (2.4 g, 38%); ^{1}H NMR (400 MHz, $CDCl_3$) δ 2.08 (4H, m, 2 × $CH_2CH_2CH_2$), 3.65 (4H, t, J = 6.0 Hz, 2 × OCH_2CH_2), 4.06 (2H, t, J = 6.2 Hz, $ArOCH_2CH_2$), 4.15 (2H, t, J = 6.3 Hz, $ArOCH_2CH_2$), 6.89 (2H, d, J = 8.3 Hz, ArH), 6.97 (3H, m, ArH), 7.28 (3H, m, ArH), 7.82 (2H, d, J = 8.4 Hz, ArH), 9.89 (1H, s, CHO).

3-Methoxy-4-[3-(3-phenoxypropoxy)propoxy]benzaldehyde (18b, R = OMe, R′ = H): colorless oil (2.5 g, 36%); ^{1}H NMR (400 MHz, $CDCl_3$) δ 2.01 (2H, quint, J = 6.4 Hz, $CH_2CH_2CH_2$), 2.13 (2H, quint, J = 6.2 Hz, $CH_2CH_2CH_2$), 3.62 (4H, m, 2 × OCH_2CH_2), 3.86 (3H, s, OCH_3), 4.02 (2H, t, J = 6.2 Hz, $ArOCH_2CH_2$), 4.18 (2H, t, J = 6.4 Hz, $ArOCH_2CH_2$),

6.91 (3H, m, ArH), 7.25 (3H, m, ArH), 7.37 (2H, m, ArH), 9.81 (1H, s, CHO).

3-Ethoxy-4-[3-(3-phenoxypropoxy)propoxy]benzaldehyde (18c, R = OEt, R′ = H): colorless oil (3.8 g, 41%); ^{1}H NMR (400 MHz, $CDCl_3$) δ 1.46 (3H, t, J = 6.9 Hz, CH_2CH_3), 2.04 (2H, quint, J = 6.1 Hz, $CH_2CH_2CH_2$), 2.13 (2H, quint, J = 6.1 Hz, $CH_2CH_2CH_2$), 3.64 (4H, m, 2 × OCH_2CH_2), 4.03 (2H, t, J = 6.1 Hz, $ArOCH_2CH_2$), 4.12 (2H, q, J = 6.9 Hz, OCH_2CH_3), 4.18 (2H, t, J = 6.1 Hz, $ArOCH_2CH_2$), 6.90 (3H, m, ArH), 7.26 (3H, m, ArH), 7.39 (2H, m, ArH), 9.82 (1H, s, CHO).

4-{3-[3-(2,4,5-Trichlorophenoxy)propoxy]propoxy}benzaldehyde (18d, R = H, R′ = 2,4,6-trichloro): colorless oil (3.9 g, 48%); ^{1}H NMR (400 MHz, $CDCl_3$) δ 2.08 (4H, m, $2xCH_2CH_2CH_2$), 3.63 (4H, m, 2 × OCH_2CH_2), 4.10 (4H, m, 2 × $ArOCH_2CH_2$), 6.94 (2H, d, J = 8.7 Hz, ArH), 7.27 (1H, s, ArH), 7.39 (1H, s, ArH), 7.80 (2H, d, J = 8.7 Hz, ArH), 9.88 (1H, s, CHO).

3-Methoxy-4-{3-[3-(2,4,5-trichlorophenoxy)propoxy]-propoxy}benzaldehyde (18e, R = OMe, R′ = 2,4,6-trichloro): colorless oil (4.6 g, 51%); ^{1}H NMR (400 MHz, $CDCl_3$) δ 2.10 (4H, m, 2 × $CH_2CH_2CH_2$), 3.65 (4H, m, 2 × OCH_2CH_2), 3.88 (3H, s, OCH_3), 4.14 (4H, m, $ArOCH_2CH_2$), 6.89 (1H, m, ArH), 6.94 (1H, s, ArH), 7.37 (2H, m, ArH), 7.42 (1H, s, ArH), 9.82 (1H, s, CHO).

3-Ethoxy-4-{3-[3-(2,4,5-trichlorophenoxy)propoxy]propoxy}benzaldehyde (18f, R = OEt, R′ = 2,4,6-trichloro): colorless oil (4.2 g, 45%); ^{1}H NMR (400 MHz, $CDCl_3$) δ 1.46 (3H, t, J = 7.0 Hz, CH_2CH_3), 2.11 (4H, m, 2 × $CH_2CH_2CH_2$), 3.66 (4H, m, 2 × OCH_2CH_2), 4.06 (2H, t, J = 6.1 Hz, $ArOCH_2CH_2$), 4.13 (2H, q, J = 7.0 Hz, OCH_2CH_3), 4.18 (2H, t, J = 6.1 Hz, $ArOCH_2CH_2$), 6.91 (1H, m, ArH), 6.94 (1H, m, ArH), 7.40 (2H, m, ArH), 7.46 (1H, s, ArH), 9.83 (1H, s, CHO).

Enzyme Preparation. The wild type and mutant pfDHFR enzymeswere expressed in *E. coli* BL21(DE3)pLysS according to the procedure previously described.[20] After disruption of the bacterial cells by a French pressure cell at 18 000 psi, the crude extract in 20 mM potassium phosphate buffer at pH 7.0, 0.1 mM EDTA, 10 mM DTT, 50 mM KCl, and 20% v/v glycerol was applied to Methotrexate-Sepharose column, and the pfDHFR was purified according to the procedure described.[15,21]

Enzyme Assays and Inhibition by Antifolates and Derivatives. The methods used for determination of pfDHFR activities and for the study of inhibition by antifolates and derivatives were described previously.[15,20] Calculation of K_i values was based on the assumption that the inhibitors compete for substrate binding to the active site of the enzyme.

Parasite Culture and Antimalarial Testing in Vitro. Four *P. falciparum* strains were used in this study. Strains TM4/8.2 (wild type DHFR) and K1CB1 (C59R + S108N) were generous gifts from S. Thaithong, Department of Biology, Faculty of Science, Chulalongkorn University; Csl-2 (C59R + S108N + I164L) was from A. Cowman WEHI, Australia, and V1/S (N51I + C59R + S108N + I164L) was from D. Kyle through MR4. These parasites were maintained continuously in human erythrocytes at 37 °C under 3% CO_2 in RPMI 1640 culture media supplemented with 25 mM HEPES, pH 7.4, 0.2% $NaHCO_3$, 40 μg/mL gentamicin, and 10% human serum.[22] In vitro antimalarial activity was determined by using [^{3}H]-hypoxanthine incorporation method [23] as described in detail elsewhere.[15,20]

Cytotoxicity tests of selected analogues against African green monkey kidney fibroblast (Vero cells), human epidermoid carcinoma (KB) cells, and human breast cancer (BC) cells were performed at the Bioassay Research Facility of the BIOTEC Center, NSTDA, according to the protocol described by Skehan et al. (1990).[24]

Molecular Modeling. Since the structures of pfDHFRs have already been solved, these enzymes were used for the molecular modeling study. The force field AM1 in the semiempirical method of the program Hyperchem 7 was employed, and the structure of small molecules (inhibitors) were geometrically optimized to a gradient of 0.001. The inhibitor was modeled as a protonated state at N1, as evidence by the NMR studies of both pfDHFR-bound and free states of pyrimethamine, of methotrexate and trimethoprim.[25,26] The inhibitor was docked into the active site of pfDHFR in which the protonated amino portion was arranged to initially occupy a position suitable for interaction with the carboxylate side chain of aspatate 54 (D54). Five-thousand steps of minimization on the complex, which included the inhibitor, NADPH, and all protein residues located within 7 Å from the inhibitor, were performed on a Silicon Graphics using the Insight II program and molecular mechanics (MM2) force field.

Acknowledgment. We thank the Bioassay Research Facility of the BIOTEC Center, NSTDA, for performing cytotoxicity tests. This research was supported by grants to Y.Y. from MMV, TDR, the European Union (INCO-DCand INCO-DEV), and the Wellcome Trust and grants from Thailand-TDR and Biodiversity Research and Training (BRT) Programs to S.K., from BIOTEC/NSTDA to Y.T., and from Thailand Graduate Institute of Science and Technology (TGIST) to C.S.

Supporting Information Available: Additional experimental data (^{1}H NMR) of all compounds not listed in the Experimental Section and the results of toxicity tests of TMP analogues to mammalian cells. This material is available free of charge via the Internet at http://pubs.acs.org.

References

(1) White, N. J. Drug resistance in Malaria. *Br. Med. Bull.* **1998**, *54*, 703−715.
(2) Morel, C. M. Reaching maturity-25 years of the TDR. *Parasitol. Today* **2000**, *16*, 503−551.
(3) Cowman, A. F.; Morry, M. J.; Biggs, B. A.; Cross, G. A.; Foote, S. J. Amino acid changes linked to pyrimethamine resistance in the dihydrofolate reductase−thymidylate synthase gene of *Plasmodium falciparum*. *Proc. Natl. Acad. Sci. U.S.A.* **1988**, *85*, 9109−9113.
(4) Peterson, D. S.; Walliker, D.; Wellems, T. E. Evidence that a point mutation in dihydrofolate reductase−thymidylate synthase confers resistance to pyrimethamine in *Plasmodium falciparum* malaria. *Proc. Natl. Acad. Sci. U.S.A.* **1988**, *85*, 9114−9118.
(5) Hyde, J. E. Mechanisms of resistance of *Plasmodium falciparum* to antimalarial drugs. *Microb. Inf.* **2002**, *4*, 165−174.
(6) Yuthavong, Y. Basis of antifolate action and resistance in malaria. *Microb. Inf.* **2002**, *4*, 175−182.
(7) Quaye, I.; Sibley, C. H. Molecular data on *Plasmodium falciparum* chloroquine and antifolate resistance: a public health tool. *Trends Parasitol.* **2002**, *18*, 184−186.
(8) Lemcke, T.; Christensen, I. T.; Jorgensen, F. S. Towards an understanding of drug resistance in malaria: Three dimensional structure of *Plasmodium falciparum* by homology building. *Bioorg. Med. Chem.* **1999**, *7*, 1003−1010.
(9) McKie, J. H.; Douglas, K. T.; Chan, C.; Roser, S. A.; Yates, R.; Read, M.; Hyde, J. E.; Dascombe, M. J.; Yuthavong, Y.; Sirawaraporn, W. Rational drug design approach for overcoming drug resistance: Application to pyrimethamine resistance in malaria. *J. Med. Chem.* **1998**, *41*, 1367−1370.
(10) Rastelli, G.; Sirawaraporn, W.; Sompornpisut, P.; Vilaivan, T.; Kamchonwongpaisan, S.; Quarrell, R.; Lowe, G.; Thebtaranonth, Y.; Yuthavong, Y. Interaction of pyrimethamine, cycloguanil, WR99210 and their analogues with *Plasmodium falciparum* dihydrofolate reductase: Structural basis of antifolate resistant. *Bioorg. Med. Chem.* **2000**, *8*, 1117−1128.
(11) Santos-Filho, O. A.; Alencastro, R. B.; Figueroa-Villar, J. D. Homology modeling of wild type and pyrimethamine/cycloguanil cross-resistant mutant type *Plasmodium falciparum* dihydrofolate reductase. A model for antimalarial chemotherapy resistance. *Biophys. Chem.* **2001**, *91*, 305−317.
(12) Warhurst, D. C. Antimalarial drug discovery: Development of inhibitors of dihydrofolate reductase active in drug resistance. *Drug Discovery Today* **1998**, *3*, 538−546.
(13) Canfield, C. J.; Milhous, W. K.; Ager, A. L.; Rossen, S. N.; Sweeney, T. R.; Lewis, N. J.; Jacobus, D. P. PS-15: a potent, orally active antimalarial from a new class of folic acid antagonists. *Am. J. Trop. Med. Hyg.* **1993**, *49*, 121−126.
(14) Hekmat-Nejad, M.; Rathod, P. K. *Plasmodium falciparum*: Kinetic interactions of WR99210 with pyrimethamine-sensitive and pyrimethamine resistant dihydrofolate reductase. *Exp. Parasitol.* **1997**, *87*, 222−228.
(15) Tarnchompoo, B.; Sirichaiwat, C.; Phupong, W.; Intaraudom, C.; Sirawaraporn, W.; Kamchonwongpaisan, S.; Vanichtanankul, J.; Thebtaranonth, Y.; Yuthavong, Y. Development of 2,4-diamino-

pyrimidines as antimalarials based on inhibition of the S108N and C59R+S108N mutants of dihydrofolate reductase from pyrimethamine-resistant *Plasmodium falciparum*. *J. Med. Chem.* **2002**, *45*, 1244−1252.
(16) Yuvaniyama, J.; Chitnumsub, P.; Kamchonwongpaisan, S.; Vanichtanankul, J.; Sirawaraporn, W.; Taylor, P.; Walkinshaw, M.; Yuthavong, Y. Insights into antifolate resistance from malarial DHFR-TS structures. *Nat. Struct. Biol.* **2003**, *10*, 357−365.
(17) Matthews, D. A.; Bolin, J. T.; Burridge, J. M.; Filman, D. T.; Volz, K. M.; Kaufman, B. T.; Beddell, C. R.; Champness, J. N.; Stammers, D. K.; Kraut, J. Refined crystal structures of *Escherichia coli* and chicken liver dihydrofolate reductase containing bound trimethoprim. *J. Biol. Chem.* **1985**, *260*, 381−391.
(18) Matthews, D. A.; Bolin, J. T.; Burridge, J. M.; Filman, D. J.; Volz, K. M.; Kraut, J. Dihydrofolate reductase: The stereochemistry of inhibitor selectivity. *J. Biol. Chem.* **1985**, *260*, 392−399.
(19) Domak, M.; Riche, C. Crystal and Molecular Structure of Polycarpine. *Acta Crystallogr., Sect. B: Struct. Crystallogr. Cryst. Chem.* **1977**, *33*, 3419−3422.
(20) Yuthavong, Y.; Vilaivan, T.; Chareonsethakul, N.; Kamchonwongpaisan, S.; Sirawaraporn, W.; Quarrell, R.; Lowe, G. Development of a lead inhibitor for the A16V+S108T mutant of dihydrofolate reductase from the cycloguanil-resistant strain (T9/94) of *Plasmodium falciparum*. *J. Med. Chem.* **2000**, *43*, 2738−2744.
(21) Sirawaraporn, W.; Prapunwattana, P.; Sirawaraporn, R.; Yuthavong, Y.; Santi, D. V. The dihydrofolate reductase domain of *Plasmodium falciparum* thymidylate synthase−dihydrofolate reductase. *J. Biol. Chem.* **1993**, *29*, 21637−21644.
(22) Trager, N.; Jensen, J. B. Human malarial parasites in continuous culture. *Science* **1976**, *193*, 673−675.
(23) Desjardins, R. E.; Canfield, C. J.; Haynes, J. D.; Chulay, J. D. Quantitative assessment of antimalarial activity in vitro by a semiautomated microdilution technique. *Antimicrob. Agents Chemother.* **1979**, *16*, 710−718.
(24) Skehan, P.; Storeng, R.; Scudiero, D.; Monks, A.; Mcmahon, J.; Vistica, D.; Warren, J. T.; Bokesch, H.; Kenney, S.; Boyd, M. R. New colorimetric cytotoxicity assay for anticancer-drug screening. *J. Natl. Cancer. Inst.* **1990**, *82*, 1107−1112.
(25) Cocco, L.; Groff, J. P.; Temple, C., Jr.; Montgomery, J. A.; London, R. E.; Matwiyoff, N. A.; Blakley, R. L. Carbon-13 nuclear magnetic resonance study of protonation of methotrexate and aminopterin bound to dihydrofolate reductase. *Biochemistry* **1981**, *20*, 3972−3978.
(26) Cocco, L.; Roth, B.; Temple, C., Jr.; Montgomery, J. A.; London, R. E.; Blakley, R. L. Protonated state of methotrexate, trimethoprim and pyrimethamine bound to dihydrofolate reductase. *Arch. Biochem. Biophys.* **1983**, *226*, 567−577.

JM0303352